

Stock structure analysis of *Upeneus vittatus* based on morphometric, meristic and otolith shape analysis along the Indian coast

Suman Nama

Central Institute of Fisheries Education

Shashi Bhushan (✉ shashi@cife.edu.in)

Central Institute of Fisheries Education

Karan Kumar Ramteke

Central Institute of Fisheries Education

Ashok Kumar Jaiswar

Central Institute of Fisheries Education

Binaya Bhusan Nayak

Central Institute of Fisheries Education

Vikash Pathak

Central Institute of Fisheries Education

Sahina Akter

Central Institute of Fisheries Education

Research Article

Keywords: Stock structure, Otolith, Marker, ShapeR, Wavelet transform, Exploitation

Posted Date: April 12th, 2022

DOI: <https://doi.org/10.21203/rs.3.rs-1426133/v1>

License:   This work is licensed under a Creative Commons Attribution 4.0 International License. [Read Full License](#)

Abstract

This study aimed to assess the stock structure of *Upeneus vittatus* from the Indian waters based on morphometric, meristic and otolith shape analysis. A total of 197 specimens were collected during '2018–2019' from the three landing centres (Mumbai, Kakinada, and Puri) along the Indian coast and otolith from each specimen were removed carefully. The contours of each otolith were investigated using the quantitative shape analysis software package ShapeR and Wavelet transform analysis model. The otolith contours were further processed for multivariate methods such as canonical analysis of principal component (CAP) and linear discriminant analysis (LDA). The CAP results showed that wavelet transform methods effectively extract otolith shape contours. The LDA of Wavelet coefficients showed an overall correct classification of 77.1%. A total of 20 morphometric and 10 meristic traits were extracted and subjected to statistical analysis. Factor analysis (FA) of morphometric variables shows first three factors together contribute 85.38% of the total variation. The first and second factors exhibited significant variation on the pre-pelvic length, Pre- pectoral length, Head length, preorbital length, caudal peduncle length and preorbital length of the fish body. Discriminant function analysis (DFA) shows correct classification rate of 69.04%. Meristic characters do not show significant variation among the sampled locations. Our findings suggest the existence of two different stocks of *U. vittatus* along the Indian coast. We need to adopt different management strategies for sustainable exploitation of the resources. The study recommends that otolith shape analysis is an efficient phenotypic marker to assess the stock structure of fishes than morphometric analysis.

Introduction

Stocks are arbitrary groups of fish large enough to be essentially self-reproducing, with members of each group having similar life history characteristics (Hilborn and Walters 2013). Discrimination of the stock is an interdisciplinary field that recognizes self-sustaining components within natural populations and is a central theme in fisheries management (Cadrin and Friedland 1999). To manage the fishery effectively, it is essential to understand a species' stock structure, how fishing effort and mortality are distributed (Begg and Waldman 1999) and design of appropriate management strategies where multiple stocks are differentially exploited (Ricker 1981). At present, a variety of phenotypic methods are applied for fish stock discrimination, such as body morphometry (Sajina et al. 2013; Cadrin et al. 2014), meristic characteristics (Meng and Stocker 1984; Turan 2004), otolith elemental composition (Geffen et al. 2011), otolith microstructure (Brophy and Danilowicz 2002), otolith shape analysis (Agüera and Brophy 2011; Libungan et al. 2015a; Lee et al. 2018) and applied markers (Schade et al. 2019).

Body morphometry is widely used among the phenotypic methods to detect the inter-and intra-specific shape variation (Lombarte and Leonart 1993) emerging from genetic and environmental milieu (Cardinale et al. 2004; Vignon and Morat 2010; Berg et al. 2018). Morphometrics is the field concerned with the study of variation in the size and shape of organisms and its co-variation with other variables (Bookstein 1990; Turan 1999) and these variations have been widely used for the delineation of fish stock (Silva 2003; Sajina et al. 2013).

Morphological characters have wide application in stock identification and have intense significance in ichthyology (Turan 1999). However, using a single set of linear landmarks is not sufficient to accurately describe the complex body shape of species because it does not capture all minor shape irregularities in

morphological features. More complex and advanced image analysis methods (such as Fourier analysis or wavelet transforms) are being suggested to address such drawbacks. Fourier analysis or wavelet transform method is an image analysis-based tool where all irregularities in otolith contour can be detected and compared on a point-by-point basis to spot where variations are produced (Parisi-Baradad et al. 2005).

Otoliths are intricate structures made of calcium carbonate and found in the inner ear of fishes. It helps in hearing, balancing and acoustic communication (Popper and Coombs 1982; Cruz and Lombarte 2004). Otoliths are extensively used in age and growth studies (Campana and Neilson 1985; Green et al. 2009), taxonomy (L'Abée-Lund and Jensen 1993; Tuset et al. 2006; Salimi et al. 2016), phylogenetic studies (Gaemers 1983; Lombarte et al. 2018; Teimori et al. 2019) and migration studies (Lord et al. 2010). Nevertheless, recently otolith shape analysis (shape contour analysis) is frequently being used to discriminate between fish stocks (Burke et al. 2008; Aguera & Brophy 2011; Libungan et al. 2015a; Wujdi et al. 2017; Moreira et al. 2019; Rashidabadi et al. 2019; Hoff et al. 2020).

Libungan et al. (2015a) first developed the ShapeR package for otolith shape analysis in the Atlantic herring (*Clupea harengus* Linnaeus, 1758) using the outline detection method and recommended for other teleost fishes. Otolith shape analysis using ShapeR package was successfully used for stock discrimination of several species like *Clupea harengus* (Libungan et al. 2015a); *Genypterus blacodes* (Ladroit et al. 2017); *Nibea albiflora* (Song et al. 2019); *Istigobius ornatus* (Sadeghi et al. 2020); *Sprattus sprattus* (Saltalamacchia et al. 2020); *Umbrina canosai* (Kikuchi et al. 2021).

U. vittatus belongs to the family Mullidae and is distributed in the Indo-Pacific and Western Atlantic Ocean (Froese and Pauly 2014). They are also distributed on both coasts of India (East and West coasts) and contribute significantly to demersal fishery resource. The total landing of goat fishes recorded was 0.2 lakh tons (CMFRI 2020). Goat fishes are generally caught by trawl net, and *U. vittatus*, *U. moluccensis* is the dominant catch along the Indian coast (CMFRI 2020). Among the goatfishes landed at Visakhapatnam, *U. vittatus* was the dominant species forming 65% of the total catch, followed by *U. sulphureus* (29%) and *U. molluccensis* (6%) (Prabha and Manjulatha 2008). Spawning of *U. vittatus* takes place from February to October, with a peak in July and October off the Visakhapatnam coast (Vivekanandan et al. 2003). *U. vittatus* feeds primarily on small crustaceans (mainly shrimps and crabs), teleostean fishes, and bivalve molluscs (Prabha and Manjulatha 2008). However, information on the stock structure and population dynamics of *U. vittatus* is comparatively weak and poorly understood in Indian water (Vivekanandan et al. 2003). This leads us to hypothesize that individuals inhabiting India's East and West coast comprise separate unit stock. To check this hypothesis present study was conducted to investigate the population structure of *U. vittatus* based on body morphometry, meristic and otolith shape analysis from three distinct areas along the Indian coast.

Materials And Methods

Collection of Samples

A total of 197 specimens of *U. vittatus* were collected from both East and West coast of India, covering the landing centre of Mumbai (MU), Kakinada (KA), and Puri (PU) from '2018–2019' (Fig. 1). The specimens were

brought to the lab in the icebox, washed properly and total length (TL cm) and weight (W gm) were recorded. Details of the sampling are given in Table 1.

Table 1

Details of the samples of *Upeneus vittatus* collected from three sampling locations along the Indian Coast.

Area	Sample number (n)	Stock ID	Geographic coordinates	Sampling year	Total length range (cm)
Mumbai	89	MU	18°54'N 72°49'E	October, 2018	10.95–18.44
Kakinada	66	KA	16°57'N 82°15'E	March, 2019	12.21–17.52
Puri	42	PU	19°81'N 85°83'E	November 2018	11.41–16.5
Total	197				

Acquisition of morphometric and meristic data

A total of 20 morphometric traits were taken using a vernier caliper closest to 0.01 mm from the left side of the specimens following standard protocol. A total of 10 meristic traits were extracted by following the widely accepted method of Hubbs and Lagler (1958). All the morphometric and meristic characters are enlisted in Tables 2 and 3 respectively. The size-dependent variation was removed for morphometric traits by adopting the widely accepted formula given by Elliott et al. (1995)

Table 2
Morphometric traits of *U vittatus* characters used for the present study.

Sl.no	Morphometric traits	Acronyms	Descriptions
1	Total length	TL	Length of the fish from anterior-most tip of the snout to the posterior-most tip of the longest lobe of the caudal fin
2	Fork length	FL	Length from the snout tip to the bifurcation of the caudal fin
3	Standard length	SL	Distance between the snout tip and the base of the caudal fin rays
4	Head length	HL	Length from the tip of the snout to the posteriormost margin of the operculum
5	Pre-orbital length	POL	Length from the tip of the snout to the anterior-most margin of the eye orbit
6	Post-orbital length	PoOL	Length from the posteriormost margin of eye orbit to the posterior-most part of the operculum
7	Eye diameter	ED	The diameter of the eye orbit along the body axis
8	First Pre-dorsal length	PDL-1	The distance from the tip of snout to the origin of the first dorsal fin
9	Second Pre-dorsal length	PDL-2	The distance from the tip of snout to the origin of the second dorsal fin
10	First dorsal fin base length	DFL-1	Length of the dorsal fin from the first origin of the fin to the insertion point of the fin
11	Second dorsal fin base length	DFL-2	Length of the dorsal fin from the second origin of the fin to the insertion point of the fin
12	Inter dorsal space	IDL	Distance between insertion point of ^{first} dorsal fin and origin of the second dorsal fin
13	Caudal peduncle depth	CPD	The minimum vertical distance across the caudal peduncle
14	Pre-pectoral length	PPcL	The distance from the tip of snout to the origin of pectoral fin
15	Pre-pelvic length	PPvL	The distance from the tip of snout to the origin of pelvic fin
16	Pre-anal fin length	PAL	The Length from the tip of snout to the origin of anal fin
17	Pectoral fin length	PFL	Length from the origin of the pectoral fin to the posterior-most tip of the fin
18	Anal fin base length	AFL	Length from the origin of first anal fin ray to the origin of the last anal fin ray
19	Caudal fin length	CFL	The length from the origin of the caudal fin to the posterior-most part of the caudal fin (total length- standard length)
20	Body depth	BD	Maximum width of the body (deepest part of the body)

Table 3

Meristic characters of *U. vittatus* used for the present study, includes mode, range, and the comparison of meristic characters with others published literature

Meristic characters	Acronym	Kakinada	Mumbai	Odisha	Fischer and Bianchi 1984	Uiblein Heemstra 2010	Ramteke et al. 2018	Saha et al. 2019
Dorsal fin spine	DFS	8	8	8	8	8	8	7
Dorsal fin rays	DFR	9	9	9	8	9	9	8
Anal fin spine	AFS	1	1	1	1	1	1	1
Anal fin rays	AFR	7	7	7	7	7	7	7
Pelvic fin spine	PeFS	1	1	1	1	1	1	1
Pelvic fin rays	PeFR	5	5	5	5	5	5	5
Pectoral fin rays	PFR	16 (15–17)	16 (15–17)	16 (15–17)	16 (15–17)	15–16	15–16	-
Lateral line scale	LLS	35 (34–38)	35 (34–36)	36 (36–38)	33–36	36–38	-	37
Gill rakers	GR	29 (27–32)	28 (27–31)	29 (27–32)	26–31	27–29	-	-
Branchiostegal rays	BSR	2	2	2	2	-	-	2

$M_s = M (L_s/L_o)^b$

where M_s is the morphometric measurement after size correction, 'M' is the original morphometric measurement, 'L_s' is the overall mean of the standard length of all the samples, 'L_o' is the standard length of the fish, and 'b' is the slope of the regression of log M on log L_o.

Data Analysis

All the transformed morphometric traits were subjected to descriptive statistics. Analysis of variance (ANOVA) was performed on morphometric and meristic characters to test for the significant difference among different stocks. The transformed morphometric measurements were subjected to principal component analysis (PCA) to reduce the redundancy among the samples. Factor analysis (FA) was performed on morphometric traits to evaluate the interrelationships among many variables and summarize the data into more minor variables. Among all the morphometric variables, 10 variables (7 from factor 1 and 3 from factor 2) showing a threshold value above 0.6 were sorted and subjected to discriminant function analysis (DFA). DFA was used to check whether individuals were correctly classified and generated a classification matrix. All the statistical analyses were done using STATISTICA 12 (Statsoft 2012).

Otolith Shape Analysis

Removal of otolith

The left sagittal otolith from 197 samples was carefully removed, washed and dipped into 1% Hydrogen Peroxide (H_2O_2) to remove adhering tissue and kept overnight to get dried. The dried otoliths were stored in plastic vials for further examination.

Image processing

All the left sagittal otoliths were examined and photographed using a Stereo zoom microscope equipped with a digital camera (Nikon SMZ1000) at 4x magnification with a reflected light PC interface. Sagittae was positioned with the concave side and the rostrum pointing to the left before taking the image (Fig. 4a). Due attention was given to maintain the excellent focus and high resolution of all the images and saved in jpeg (*jpg) format.

Shape Analysis

Several statistical functions have been followed in the program R to evaluate the variation of otolith shape among the population (Team 2013). Otolith images were read by R programming language using the package jpeg (Urbanek S 2014). Outlines of each otolith were extracted from the images (Fig. 4b) using the "ShapeR" package (Libungan and Pálsson 2015). The shape of each otolith was recorded as a matrix of x and y coordinates by horizontal rotation of all otoliths along their longest axis. To reduce the pixel noise, all the detected outlines were smoothed. Radii were drawn at equal intervals from the centroid of otolith to the different coordinates using the radius function in R (Claude 2008). The length of these radii acts as a univariate shape descriptor. Wavelet shape coefficients were obtained by discrete Wavelet transform methods using Wave thresh package (Libungan and Pálsson 2015; Nason 2016).

Mean otolith shape analysis

Variation of otolith shape among populations was assessed visually by plotting the average otolith shape for each population using the outlines of the normalized Wavelet coefficients (Fig. 5). To evaluate which areas and coefficients of the otolith shape contribute the most distinction among populations, mean shape coefficients and their standard deviation were plotted against the angle of the outline using Wavelet transform coefficients (Libungan and Pálsson 2015) (Fig. 6). The quality of the Wavelet coefficients was estimated by using a maximum number of 15 harmonics, comparing how it deviates from the otolith outline (Libungan and Pálsson 2015).

Multivariate statistical analysis

Canonical analysis of principal coordinates (CAP) was applied on the Wavelet coefficients to find the shape variation among the populations (Anderson and Willis 2003) using the capscale function in the vegan package (Oksanen et al. 2014). The average constrained ordination in each stock was graphically evaluated along the first two canonical axes, CAP1 and CAP2, with shape descriptors. An ANOVA-like permutation test (over 1000 permutations) was used for CAP to assess the significance constraints using the vegan package in R (Oksanen et al. 201) since this is a potent test and does not require normality for significance in canonical axes (Legendre

et al. 2011). Linear Discriminant Analysis (LDA) was applied on the standardized Wavelet coefficients from each group to estimate the otolith shape classification success rate (Libungan and Pálsson 2015) with 'leave-one-out' cross-validation using the errorest function in the ipred package (Peters and Hothorn 2013). All statistical analysis was performed in the R software (R Core Team 2013).

Results

Traditional morphometric analysis

The descriptive statistics morphometric variables are given in Table 4. ANOVA of the transformed morphometric variables showed significant variation among the locations ($p < 0.05$). Most variations were observed in the anterior and posterior portions of the fish body. The DFA of the morphometric measurements suggests that all samples were well separated from each other and there was limited mixing among the stocks. The total length of *U. vittatus* was ranged from 10.95 to 21.44 cm with the coefficients of variation (CV) of 10.85. The largest specimen was reported for a female from the Mumbai coast (21.44 cm). The first two principal components obtained from PCA of morphometric variables explained 83.94% of total variation with the eigenvalues of 16.39 and 1.23 respectively.

Table 4
Overall descriptive statistics of morphometric traits

Traits	Mean	Mini	Maxi	C.V(%)	S. D
TL	14.47	10.95	21.44	10.85	1.57
SL	11.98	8.97	17.77	11.11	1.33
FL	12.95	9.83	18.94	10.84	1.40
HL	3.27	2.40	5.01	12.87	0.42
POL	1.00	0.62	1.65	17.09	0.17
ED	0.88	0.60	1.38	14.51	0.12
PoOL	1.63	1.16	2.51	12.99	0.21
PDL-1	4.76	3.45	7.28	11.84	0.56
DFL-1	2.06	1.46	3.42	15.28	0.31
IDL	1.56	1.07	2.68	14.57	0.22
PDL-2	8.03	6.05	12.18	11.17	0.89
DFL-2	1.67	0.81	2.56	13.90	0.23
PpCL	3.53	2.57	5.24	12.77	0.45
PpAL	2.95	1.92	4.63	13.25	0.39
PPvl	3.77	2.78	5.95	13.26	0.50
PAL	8.12	6.06	12.45	11.59	0.94
AFL	1.39	0.95	2.01	12.14	0.16
BW	3.34	2.28	5.09	12.81	0.42
CFL	2.96	2.24	4.57	12.37	0.36
CPD	1.33	0.95	1.98	13.04	0.17

In the FA, morphometric characters with a factor loading above 0.6 on any of the first two factors were selected for subsequent DFA. The morphometric traits with meaningful loading on the first factor (Fig. 2) were the first pre-dorsal length, 2nd pre-dorsal length, pre-pelvic length, pre-pectoral length, head length, preorbital length and pectoral fin length and on the second factor (Fig. 3) were total length, first dorsal fin base length and caudal fin length (Table 5). The cross-validation of the DFA showed an overall correct classification rate of 69.04%, where the highest and lowest classification was observed in Mumbai and Puri populations respectively. The individuals were correctly classified in the stocks as MU-75.28%, KA-66.66%, and PU-59.52% (Table 6).

Table 5
 Factor loadings of morphometric traits (Varimax raw)
 Extraction: Principal components (Marked loadings are
 > .600000).

Variables	Factor - 1	Factor - 2
1st pre-dorsal length	-0.821081	-0.107005
2nd predorsal length	-0.701904	-0.060169
Total length	0.137469	-0.600788
Fork length	0.169768	-0.477630
Pre-anal length	-0.564335	0.008894
Pre-pelvic length	-0.738083	-0.101832
Pre- pectoral length	-0.853396	-0.051942
Head length	-0.830206	-0.095719
preorbital length	-0.709087	-0.149075
1st dorsal fin base length	-0.089082	-0.600935
Inter dorsal length	0.117958	0.492964
Body width	-0.407220	-0.183945
2nd dorsal fin base length	0.359516	-0.492415
Caudal fin length	0.321475	-0.633603
Caudal peduncle width	0.123115	-0.488426
Anal fin base length	0.453249	-0.352315
Postorbital length	-0.340378	-0.278632
Pectoral fin length	-0.737169	-0.071676
Eye dia	0.141915	0.001515
Expl.Var	5.318416	2.376037
Prp.Totl	0.279917	0.125055

Table 6
Classification matrix of morphometric variables from different stocks in
stepwise discriminant analysis

Location	Kakinada	Mumbai	Odisha	Total	(%) classified
Mumbai	67	11	11	89	75.28
Puri	11	25	6	42	59.52
Kakinada	12	10	44	66	66.66
Total	90	46	61	197	69.04

Out of 10 meristic traits, 6 traits, such as dorsal fin spines, branchiostegal rays, pelvic fin spines, pelvic fin soft rays, anal fin spines, and anal fin rays, showed no variation among all the locations. The lateral line scales showed the highest standard deviation, followed by gill rakers and pectoral fin rays. The analysis of meristic traits revealed that *U. vittatus* has 8 dorsal fin spines, 9 dorsal-fin rays, 1 pelvic fin spine, and 7 pelvic fin rays, 1 anal fin spines, 7 anal fin rays, 15–17 pectoral-fin rays, 34–38 lateral line scales, 27–32 gill rakers, and 2 branchiostegal rays (Table 3). Kruskal Wallis test revealed no significant difference among the sampling stations for meristic traits ($p > 0.05$).

Otolith shape analysis

Otoliths of Yellow striped" goatfish (*U. vittatus*) are elliptic in shape; margins are conspicuous, anterior regions peaked, and posterior margins are oblique irregular (Ramteke et al. 2018). All these morphometric features of the otolith were evaluated using the wavelet transform coefficients and proven to be potent tools in the stock discrimination of *U. vittatus*. The results of the ANOVA-like permutation test shows that the mean values of the shape (detected otolith outline) differ significantly between the East and West coast of India ($P < 0.005$) and maximum variation was observed in the postrostrum and pararostrum regions of the otolith (Fig. 5). The wavelet coefficient mean and interclass correlation (ICC) were used for quantitative analysis of the otolith shape differences in terms of polar angles and it pinpoint the main differences in the otolith among the localities (Fig. 6).

A high level of shape variation in the Wavelet coefficients was observed between at 0° – 100° and 240° – 320° angle. Further investigation of the mean shapes shows that the rostrum and antirostrum regions of the otolith do not show significant variation among the sampling stations but dorsal and ventral edges of otolith show shape variation (Fig. 5). For modelling, the otolith contour deviation from the outline was estimated with Wavelet levels. Deviation from the outline decreased sharply as the Wavelet level (the number of coefficients) increased. The first five coefficients showed 98.5% of the deviation (Fig. 7). Otolith shape of MU populations move towards the centroid of otolith in the pararostrum region and outward in the postrostrum region. In comparison, the KA and PU population shows a slight variation in the pararostrum and postrostrum regions. Overlapping was observed among all the sampling groups in the rostrum and antirostrum region (angle 130° – 180°). In the ventral edge (angle 240° – 320°), the distance from the otolith centroid was higher for PU and KA samples than for MU samples.

The canonical analysis of the principal (CAP) from length-standardized wavelet coefficients results showed significant variation in otolith shape among the three sampling stations (ANOVA, $p < 0.001$). Where first (CAP1)

and second (CAP2) axis shows 97.8% and 2.2% of shape variation, respectively (Fig. 8). The first discriminating axis (CAP1) shows that the otolith shape of the MU population differs from KA and PU populations. In contrast, the otolith shape of KA deviated from others in the second discriminating axis (CAP2). It indicates that most variables in otolith shape contour were observed in MU samples among the study sites.

Cross validated classification matrix of LDA from three different locations gave an overall classification success rate of 77.1%. The sampling sites' classification accuracy was 86.51%, 69.04%, and 75.75% for Mumbai, Puri and Kakinada populations, respectively (Table 7). Maximum misclassification was observed in the Puri (PU) population with 30.96% and the minimum was in the MU population. In general, the analysis revealed that the contours of the sagittal otolith differed markedly and suggested the existence of two different stocks of *U. vittatus* along the Indian coast.

Table 7
Cross validated classification success results based on Linear Discriminant Analysis (LDA) of standardized Wavelet coefficients of *U. vittatus* populations from the three distinct locations.

Locations	Number of otolith samples used				Classification %
	Mumbai	Puri	Kakinada	Total	
Mumbai	77	9	3	89	86.51
Puri	8	29	5	42	69.04
Kakinada	7	9	50	66	75.75
Total	92	47	58	197	77.1

Discussion

Morphometric and meristic characters

The traditional morphometric and meristic methods, along with otolith shape analysis, were used to discriminate the stocks structure of *U. vittatus*. Both univariate and multivariate statistical analyses were used to check the otolith shape variation among the populations. This study revealed significant variations among the populations based on the otolith shape analysis, traditional morphometric and meristic characters. Studies based on morphometry and meristic analysis have been carried out for stock identification in several species, such as *Megalaspis cordyla* (Sajina et al. 2011), *Nemipterus japonicus* (Sreekanth et al. 2015), *Nemipterus randalli* (Sri Hari et al. 2020).

Factor analysis of the morphometric traits showed that factor 1 shows variation in the anterior portion and factor 2 is in the posterior portion of the fish body. The mean caudal peduncle depth of specimens collected from India's east and west coast was 1.54 cm and 1.25 cm respectively, indicating well-developed caudal peduncle in the east coast populations than the west coast. Variation in the caudal peduncle region could be due to unique hydrographical conditions on both the coast. Several studies reported significant differences in the caudal peduncle region of the fish body along the Indian coast (Sajina et al. 2013; Sreekanth et al. 2015; Sri Hari et al. 2020). The turbidity of the Bay of Bengal is generally much higher than the Arabian sea (Kumar et al.

2001) as the Bay of Bengal receives a heavy riverine discharge. Because of high turbidity, the fishes might have to swim more to find suitable food items, leading to a strong caudal peduncle region. Imre et al. (2002) studied the population of brook charr (*Salvelinus fontinalis*) from different microhabitats with the difference in the velocity of the water. They found that those highly turbulent species have a deeper and well-developed caudal peduncle.

The mean total length of fishes studied from Mumbai, Kakinada, and Odisha was 15.56 cm, 14.03 cm and 13.96 cm, respectively. The variation in the total length may be due to the abundance of food and higher feeding intensity. Kumar et al. (2009) stated that continuous upwelling of cold nutrient-rich water, wind-driven mixing, and lateral advection had enhanced the productivity of the Arabian sea. In contrast, the biological productivity of the Bay of Bengal is considered low (Kumar et al. 2001). The supportive environmental condition along with continuous availability of sufficient quantity of food items lead to the higher growth performance of Arabian sea populations. The mean head length was higher for the Mumbai population (3.61 cm) and the lowest for the Odisha population (3.01 cm). The difference in the morphometric characters between the samples may be due to habitat changes, whereas the variation in relative head length could be related to the size of prey (Gatz 1979). The dorsal fin plays a crucial role in the swimming patterns of coral reef fishes (Korsmeyer 2002). *U. vittatus* is a reef-dwelling fish. The variation in dorsal fin length may be due to different current patterns and velocities existing in India's coast.

Otolith Shape Analysis

Multivariate analysis of the discrete Wavelet transforms successfully characterized individuals from India's East and West coast. The Wavelet transform is proven to be an effective tool in otolith shape analysis because it can detect otolith contour outlines which contribute significantly to overall shape variation (Postrostrum and Pararostrum in the present finding). The result of the present study shows the usefulness of otolith shape analysis in the possible identification of two different stocks of *U. vittatus* along the Indian coast. However, the vast geographical distance between India's East and West coast may be a barrier for larval dispersion between these areas and form the different genetic stock. In this study, the specimens with a total length of above 10 cm were used to ensure all 197 specimens were adult to avoid the confounding effect of allometric growth on otolith shape (Cardinale et al. 2004). The use of otolith shape analysis might be of imperceptible value to discriminate the stock if applied to sexually immature specimens (Campana & Casselman 1993). Elliptic Fourier or Wavelet transform functions use harmonics to describe the shape of the otolith (Parisi-Baradad et al. 2005). Each harmonic amplitude represents a shape characteristic such as elongation and triangularity (Bird 1986).

The environmental and genetic factors are responsible for otolith shape differences (Lombarte & Lleonart 1993; Cardinale et al. 2004; Teacher et al. 2013), leading to the distinctive features of each stock (Friedland and Reddin 1994; Begg and Waldman 1999). Several studies revealed that local environmental conditions play a crucial role in the growth of fishes (Silva et al. 2008; Veron et al. 2020) and otolith shape variation (Cardinale et al. 2004; Vignon 2012). Vignon & Morat (2010) stated that the species-specific otoliths are genetically regulated, while environmental effects on otolith shape are mainly expressed at an intraspecific level. This indicates that the otolith's shape can differ in the absence of any growth-related differences if genetic differences exist between populations (Galley et al. 2006).

So, the individuals who breed and grow in different environmental conditions are expected to have unique morphology and growth rates and form distinct demographic stocks. East and West coast of India experienced different environmental conditions throughout the year. So, the observed variation in the otolith shape of *U. vittatus* may be due to environmental differences among the sampling areas or may have a genetic basis. Truss morphometric analysis of *U. vittatus* along the Indian coast indicates that the unique demographic features in India's East and West coast may attribute to separate stock (Nama et al. 2022).

Furthermore, the LDA showed that Mumbai samples significantly differed from Kakinada and Puri populations, forming a separate cluster suggesting that the individuals captured were exposed to different environmental conditions. The classification matrix of shape contours derived from the Wavelet transform analysis of otolith showed a separation of populations collected from three different locations along the Indian coast. One possible explanation for those specific differences is related to the dominant oceanographic processes along the west coast of India. Habitat temperature is a vital environmental factor that affects the growth of fish and otolith morphometry. Neat et al. (2008) investigated that 2°C changes in water temperature can lead to variation in opacity and daily increments of otoliths width in Atlantic cod (*Gadus morhua*). Variation in otolith shape may occur due to changes in water column temperature along the latitudinal gradient (Castro et al. 2015; Cuevas et al 2019). It is supported by the theory given by Lombarte & Lieonart (1993) otolith shape can be varied among the populations that might have grown up at the same temperature and growing conditions like other morphometric traits, which reflects the combined effect of genetic variation and local environmental condition, such as water depth, salinity, pressure, and water temperature.

East and West coast of India exhibited wide seasonal temperature fluctuation of its surface water. Moreover, salinity is higher on the west coast of India than on the east coast, most probably due to the heavy discharge of freshwater from the major rivers into the east coast. This might be the probable reason for the otolith shape variation and sampling locations. Different multivariate analyses of the Wavelet shape descriptors, i.e., permutation tests, showed significantly different dorsal and ventral parts than in other locations. Food availability in that area may be the possible attribute for the fastest deposition of otolith increments. Food availability in the Arabian Sea is much higher than in the Bay of Bengal. Because seasonal upwelling of cold, nutrient-rich waters along the western coast of India contribute significantly to primary production (Panikkar and Jayaraman 1996). Thus, different growth rates of fishes contribute to the otolith shape variations among the observed populations. The protein content of food items consumed by fish directly affects otolith development. The fish's growth rate is directly related to the otolith shape (Gauldie and Nelson 1990) because faster-growing fishes usually have daily ring deposition, whereas fewer rings are observed in slow-growing fishes (Geffen 1982; Fox et al. 2003). Thus, differences in the consumption of type and quality of food items result in differences in otolith shape (Mille et al. 2016). Fluctuations of the diet in terms of quantity and frequency also determine otolith's shape significantly over a short period (Gagliano and McCormick 2004). A similar study conducted by Hussy (2008) stated that the size and number of lobes formed in the otolith are greatly influenced by feeding. However, otolith shape development depends on fed consumption and fishes' growth rate. Therefore, differences in food items consumed by Yellow striped" goatfish in the different environmental conditions may affect the shape of the otolith.

Conclusions

The present study based on traditional morphometric and otolith shape analysis revealed a significant variation among the population, indicating two separate stocks of *U. vittatus* along the Indian coast. We need to adopt different management strategies to ensure sustainable uses of genetic resources and maintain genetic diversity (Begg & Waldman 1999). Therefore, we could conclude that the observed otolith shape variation in *U. vittatus* between India's East and West coast may be due to internal factors like age, condition, reproduction, or ecological differences such as water quality, temperature, and salinity. This indicates that otolith shape analysis can be a potent, cheaper, and more efficient tool than morphometric analysis to discriminate the fish stock and it can be used widely for effective manage fisheries resources (Cardinale et al. 2004; Tracey et al. 2006). A further combined investigation based on molecular techniques such as mtDNA, microsatellite marker, and otolith elemental composition analysis is required to understand clearly the stock structure of "Yellow striped" goatfish (*U. vittatus*) along the Indian coast. A failure to accurately identify genetic stocks may lead to poor management of resources and causes overexploitation of some stocks.

Declarations

Acknowledgments

The authors are thankful to the Director, ICAR-Central Institute of Fisheries Education, Mumbai, for carrying out this work. The first author is grateful to the (ICAR) Indian Council of Agricultural Research, New Delhi, India, for providing a (JRF) Junior Research Fellowship to carry out the research work.

Authors' contributions

Suman Nama: Planning of work, specimens' collection, data analysis, manuscript drafting.

Shashi Bhushan: Designed the overall work, final approval for manuscript submission.

Karan Kumar Ramteke: Data analysis, manuscript checking.

Ashok Kumar Jaiswar: Manuscript edition, checking of manuscript.

Binaya Bhusan Nayak: Manuscript checking

Vikash Pathak: Data analysis drafting.

Sahina Akter: Specimen's collection and dissection.

Availability of data and materials

Data will be available based on request.

Funding

The research was conducted with the fund support of Indian Council of Agricultural Research (ICAR), New Delhi.

Ethics approval consent to participate: Not applicable

Declarations Ethics approval and consent to participate: The manuscript is not submitted in any other journal. This manuscript does not involve the use of any live animal. Fish samples directly obtained from the commercial catches were used.

Consent to participate: Not applicable.

Consent for publication: The approval for submitting manuscript received from ICAR- Central Institute of Fisheries Education.

Competing interests: The authors declared that there is no competing interest for this publication.

References

1. Agüera A, Brophy D (2011) Use of sagittal otolith shape analysis to discriminate Northeast Atlantic and Western Mediterranean stocks of Atlantic saury, *Scomberesox saurus saurus* (Walbaum). *Fish Res* 110(3):465–471
2. Anderson MJ, Willis TJ (2003) Canonical analysis of principal coordinates: a useful method of constrained ordination for ecology. *Ecol* 84(2):511–525
3. Begg GA, Waldman JR (1999) An holistic approach to fish stock identification. *Fish Res* 43(1–3):35–44
4. Berg F, Almeland OW, Skadal J, Slotte A, Andersson L, Folkvord A (2018) Genetic factors have a major effect on growth, number of vertebrae and otolith shape in Atlantic herring (*Clupea harengus*). *PLoS ONE* 13(1):e0190995
5. Bird JL, Eppler DT, Checkley DM Jr (1986) Comparisons of herring otoliths using Fourier series shape analysis. *Can J Fish Aquat Sci* 43(6):1228–1234
6. Bookstein FL (1990) Introduction to methods for landmark data. In *Proceedings of the Michigan morphometrics workshop* Ann Arbor: The University of Michigan museum of zoology. 2: 215–226
7. Brophy D, Danilowicz BS (2002) Tracing populations of Atlantic herring (*Clupea harengus* L.) in the Irish and Celtic Seas using otolith microstructure. *ICES J Mar Sci* 59(6):1305–1313
8. Burke N, Brophy D, King PA (2008) Otolith shape analysis: its application for discriminating between stocks of Irish Sea and Celtic Sea herring (*Clupea harengus*) in the Irish Sea. *ICES J Mar Sci* 65(9):1670–1675
9. Cadrin SX, Friedland KD (1999) The utility of image processing techniques for morphometric analysis and stock identification. *Fish Res* 43(1–3):129–139
10. Cadrin SX, Kerr LA, Mariani S (2014) Interdisciplinary evaluation of spatial population structure for definition of fishery management units. In *Stock Identification Methods*, Academic Press, pp 535–552
11. Campana SE, Casselman JM (1993) Stock discrimination using otolith shape analysis. *Can J Fish Aquat Sci* 50(5):1062–1083
12. Campana SE, Neilson JD (1985) Microstructure of fish otoliths. *Can J Fish Aquat Sci* 42(5):1014–1032
13. Cardinale M, Doering-Arjes P, Kastowsky M, Mosegaard H (2004) Effects of sex, stock, and environment on the shape of known-age Atlantic cod (*Gadus morhua*) otoliths. *Can J Fish Aquat Sci* 61(2):158–167
14. Castro L, Soto S, Llanos A, Pérez I, Cubillos L, Alarcón R, Claramunt G, Herrera G, Parada C, Escalona E, Barrientos P (2015) Identificación de zonas de desove y estadios tempranos de pelágicos pequeños en

- aguas interiores de la X y XI Regiones. Technical Report FIP. 2013-17
15. Claude J (2008) Morphometrics with R. Springer Science & Business Media
 16. CMFRI (2020) Marine fish landings in India 2019, Technical Report. ICAR-Central Marine Fisheries Research Institute. Kochi, India. p 1–15
 17. Core Team RCTR (2013) R: A language and environment for statistical computing. R Foundation for statistical computing, Vienna
 18. Cruz A, Lombarte A (2004) Otolith size and its relationship with colour patterns and sound production. *J Fish Biol* 65(6):1512–1525
 19. Cuevas LA, Tapia FJ, Iriarte JL, González HE, Silva N, Vargas CA (2019) Interplay between freshwater discharge and oceanic waters modulates phytoplankton size-structure in fjords and channel systems of the Chilean Patagonia. *Prog Ocean* 173:103–113
 20. Elliott NG, Haskard K, Koslow JA (1995) Morphometric analysis of orange roughy (*Hoplostethus atlanticus*) off the continental slope of southern Australia. *J fish biol* 46(2):202–220
 21. Fischer W, Bianchi G (1984) FAO species identification sheets for fishery purposes. Western Indian Ocean; (Fishing Area 51). Rome, Food and Agricultural Organization of the United Nations, vols 1–6
 22. Fox CJ, Folkvord A, Geffen AJ (2003) Otolith micro-increment formation in herring *Clupea harengus* larvae in relation to growth rate. *Mar Ecol Prog Ser* 264:83–94
 23. Friedland KD, Reddin DG (1994) Use of otolith morphology in stock discriminations of Atlantic salmon (*Salmo salar*). *Can J Fish Aquat Sci* 51(1):91–98
 24. Froese R, Pauly D (2014) Fish Base. World Wide Web electronic publication. www.fishbase.org, version (06/2011). Accessed on 12 October 2018
 25. Gaemers PA (1983) Taxonomic position of the Cichlidae (Pisces, Perciformes) as demonstrated by the morphology of their otoliths. *Neth J Zool* 34(4):566–595
 26. Gagliano M, McCormick MI (2004) Feeding history influences otolith shape in tropical fish. *Mar Ecol Prog Ser* 278:291–296
 27. Galley EA, Wright PJ, Gibb FM (2006) Combined methods of otolith shape analysis improve identification of spawning areas of Atlantic cod. *ICES J Mar Sci* 63(9):1710–1717
 28. Gatz Jr (1979) Community organization in fishes as indicated by morphological features. *Ecology* 60(4):711–718
 29. Gauldie RW, Nelson DGA (1990) Otolith growth in fishes. *Comp Biochem Physiol Part A: Physiol* 97(2):119–135
 30. Geffen AJ, Nash RD, Dickey-Collas M (2011) Characterization of herring populations west of the British Isles: an investigation of mixing based on otolith microchemistry. *ICES J of Mar Sci* 68(7):1447–1458
 31. Geffen AJ (1982) Otolith ring deposition in relation to growth rate in herring (*Clupea harengus*) and turbot (*Scophthalmus maximus*) larvae. *Mar Biol* 71(3):317–326
 32. Green BS, Mapstone BD, Carlos G, Begg GA (eds) (2009) Tropical fish otoliths: information for assessment, management and ecology, vol 11. Springer Science & Business Media
 33. Hilborn R, Walters CJ (2013) Quantitative fisheries stock assessment: choice, dynamics and uncertainty. Springer Science & Business Media

34. Hoff NT, Dias JF, Zani-Teixeira MDL, Correia AT (2020) Spatio-temporal evaluation of the population structure of the bigtooth corvina *Isopisthus parvipinnis* from Southwest Atlantic Ocean using otolith shape signatures. *J Appl Ichthyol* 36(4):439–450
35. Hubbs CL, Lagler KL (1958) *Fishes of the Great Lakes region*, 2nd edn. Cranbrook Institute of Science Bulletin, Michigan, USA, p 213
36. Hussy K, Mosegaard H (2004) Atlantic cod (*Gadus morhua*) growth and otolith accretion characteristics modelled in a bioenergetics context. *Can J Fish Aquat Sci* 61(6):1021–1031
37. Imre I, McLaughlin RL, Noakes DLG (2002) Phenotypic plasticity in brook charr: changes in caudal fin induced by water flow. *J Fish Biol* 61(5):1171–1181
38. Kikuchi E, Cardoso LG, Canel D, Timi JT, Haimovici M (2021) Using growth rates and otolith shape to identify the population structure of *Umbrina canosai* (Sciaenidae) from the Southwestern Atlantic. *Mar Biol Res* 7(3):272–285
39. Korsmeyer KE, Steffensen JF, Herskin J (2002) Energetics of median and paired fin swimming, body and caudal fin swimming, and gait transition in parrotfish (*Scarus schlegelii*) and triggerfish (*Rhinecanthus aculeatus*). *J exper biol* 205(9):1253–1263
40. Kumar SP, Madhuratap M, Kumar MD, Muraleedharan PM, De Souza SN, Gauns M, Sarma VSS (2001) High biological productivity in the central Arabian Sea during the summer monsoon driven by Ekman pumping and lateral advection. *Curr Sci* 81(12):1633–1638
41. L'Abée-Lund JH, Jensen AJ (1993) Otoliths as natural tags in the systematics of salmonids. *Environ Biol Fish* 36(4):389–393
42. Ladroit Y, Maolagáin CO, Horn PL (2017) An investigation of otolith shape analysis as a tool to determine stock structure of ling (*Genypterus blacodes*). *New Z Fisheries Assess Rep* 24:16
43. Lee B, Brewin PE, Brickle P, Randhawa H (2018) Use of otolith shape to inform stock structure in Patagonian toothfish (*Dissostichus eleginoides*) in the south-western Atlantic. *Mar Fresh Res* 69(8):1238–1247
44. Legendre P, Oksanen J, Ter Braak CJF (2011) Testing the significance of canonical axes in redundancy analysis. *Methods Ecol Evol* 2:269–277
45. Libungan LA, Óskarsson GJ, Slotte A, Jacobsen JA, Pálsson S (2015) Otolith shape: a population marker for Atlantic herring (*Clupea harengus*). *J Fish Biol* 86(4):1377–1395
46. Libungan LA, Pálsson S (2015) ShapeR: an R package to study otolith shape variation among fish populations. *PLoS ONE* 10(3):e0121102
47. Libungan LA, Slotte A, Husebø Å, Godiksen JA, Pálsson S (2015) Latitudinal gradient in otolith shape among local populations of Atlantic herring (*Clupea harengus*) in Norway. *PLoS ONE* 10(6):e0130847
48. Lombarte A, Leonart (1993) Otolith size changes related with body growth, habitat depth and temperature. *Environ Biol Fish* 37(3):297–306
49. Lombarte A, Miletić M, Kovačić M, Otero-Ferrer JL, Tuset VM (2018) Identifying sagittal otoliths of Mediterranean Sea gobies: variability among phylogenetic lineages. *J fish biol* 92(6):1768–1787
50. Lord C, Brun C, Hauteceur M, Keith P (2010) Insights on endemism: comparison of the duration of the marine larval phase estimated by otolith microstructural analysis of three amphidromous Sicyopterus

- species (Gobioidei: Sicydiinae) from Vanuatu and New Caledonia. *Ecol fresh fish* 19(1):26–38
51. Meng HJ, Stocker M (1984) An evaluation of morphometrics and meristics for stock separation of Pacific herring (*Clupea harengus pallasii*). *Can J Fish Aquat Sci* 41(3):414–422
 52. Mille T, Mahe K, Cachera M, Villanueva MC, de Pontual H, Ernande B (2016) Diet is correlated with otolith shape in marine fish. *Mar Ecol Prog Ser* 555:167–184
 53. Moreira C, Froufe E, Sial AN, Caeiro A, Vaz-Pires P, Correia AT (2018) Population structure of the blue jack mackerel (*Trachurus picturatus*) in the NE Atlantic inferred from otolith microchemistry. *Fish Res* 197:113–122
 54. Nama S, Bhushan S, Ramteke KK, Jaiswar AK, Srihari M (2022) Stock structure analysis of Yellow striped goatfish, *Upeneus vittatus* (Forsskal, 1775) based on truss morphometric analysis along the Indian coast. *Ira J Fish Sci* 21(1):93–103
 55. Nason G (2016) Package 'wavethresh': wavelets statistics and transforms. Springer, New York (NY)
 56. Neat FC, Wright PJ, Fryer RJ (2008) Temperature effects on otolith pattern formation in Atlantic cod *Gadus morhua*. *J Fish Biol* 73(10):2527–2541
 57. Oksanen J, Blanchet FG, Kindt R, Legendre P, Minchin PR, O'Hara RB, Simpson GL, Solymos P, Stevens MHH, Wagner H (2014) *Vegan: Community Ecology Package*. R Package Version. 2.2-0. <http://CRAN.Rproject.org/package=vegan>
 58. Panikkar NK, Jayaraman R (1966) Biological and oceanographic differences between the Arabian Sea and the Bay of Bengal as observed from the Indian region. *Pro Ind Aca Sci* 64(5):231–240
 59. Parisi-Baradad V, Lombarte A, García-Ladona E, Cabestany J, Piera J, Chic O (2005) Otolith shape contour analysis using affine transformation invariant wavelet transforms and curvature scale space representation. *Mar fresh res* 56(5):795–804
 60. Peters A, Hothorn T (2013) *ipred: Improved Predictors*, version 0.9–3. R package
 61. Popper AN, Coombs S (1982) The morphology and evolution of the ear in Actinopterygian fishes. *Ame Zool* 22(2):311–328
 62. Prabha YS, Manjulatha C (2008) Food and feeding habits of *Upeneus vittatus* (Forsskal, 1775) from visakhapatnam coast (Andhra Pradesh) of India. *Int J Zool Res* 4:59–63
 63. Prasanna Kumar S, Narvekar J, Nuncio M, Gauns M, Sardesai S (2009) What drives the biological productivity of the northern Indian Ocean? Washington DC American Geophysical Union. *Geophys Monogr Ser* 185:33–56
 64. Ramteke KK, Landge AJ, Jaiswar AK, Chakraborty SK, Deshmuke D, Renjith RK (2018) Taxonomic differentiation of goatfishes (Family-Mullidae) based on morphological traits and hard parts. *Ind J Geo mar sci* 47(02):381–389
 65. Rashidabadi F, Abdoli A, Tajbakhsh F, Nejat F, Aviglian E (2020) Unravelling the stock structure of the Persian brown trout by otolith and scale shape. *J fish biol* 96(2):307–315
 66. Ricker WE (1981) Changes in the average size and average age of Pacific salmon. *Can J Fish Aquat Sci* 38(12):1636–1656
 67. Sadeghi R, Esmaeili HR, Zarei F, Reichenbacher B (2020) Population structure of the ornate goby, *Istigobius ornatus* (Teleostei: Gobiidae), in the Persian Gulf and Oman Sea as determined by otolith shape variation

using ShapeR. Environ Biol Fish 103(10):1217–1230

68. Saha S, Sehrin S, Al Masud A, Habib KA, Sarker A, Baki MA (2019) New Records of the Goatfish, *Upeneus Vittatus* (Forsskal 1775) and *Upeneus Supravittatus* (Uiblein and Heemstra 2010) (Perciformes, Mullidae), From Saint Martin's Island in the Bay of Bengal, Bangladesh. J Asia Soc Bangl 45(2):161–173
69. Sajina AM, Chakrabort SK, Jaiswar AK, Pazhayamadom DG, Sudheesan D (2011) Stock structure analysis of *Megalaspis cordyla* (Linnaeus, 1758) along the Indian coast based on truss network analysis. Fish Res 108(1):100–105
70. Sajina AM, Chakrabort SK, Jaiswar AK, Sudheesan D (2013) Morphometric and meristic analyses of horse mackerel, *Megalaspis cordyla* (Linnaeus, 1758) populations along the Indian coast. Ind J Fish 60(4):27–34
71. Salimi N, Loh KH, Dhillon SK, Chong VC (2016) Fully-automated identification of fish species based on otolith contour: using short-time Fourier transform and discriminant analysis (STFT-DA). PeerJ 4:e1664
72. Saltalamacchia F, Berg F, Casini M, Davies JC, Bartolino V (2022) Population structure of European sprat (*Sprattus sprattus*) in the Greater North Sea ecoregion revealed by otolith shape analysis. Fish Res 245:106131
73. Schade FM, Weist P, Krumme U (2019) Evaluation of four stock discrimination methods to assign individuals from mixed-stock fisheries using genetically validated baseline samples. Mar Ecol Prog Ser 627:125–139
74. Silva A, Carrera P, Massé J, Uriarte A, Santos MB, Oliveira PB, Soares E, Porteiro C, Stratoudakis Y (2008) Geographic variability of sardine growth across the Northeastern Atlantic and the Mediterranean Sea. Fish Res 90(1–3):56–69
75. Silva A (2003) Morphometric variation among sardine (*Sardina pilchardus*) populations from the northeastern Atlantic and the western Mediterranean. ICES J Mar Sci 60(6):1352–1360
76. Song J, Zhao B, Liu J, Cao L, Dou S (2019) Comparative study of otolith and sulcus morphology for stock discrimination of yellow drum along the Chinese coast. J Ocen Lim 37(4):1430–1439
77. Sreekanth GB, Chakraborty SK, Jaiswar AK, Renjith RK, Kumar R, Sandeep KP, Vaisakh G, Ail SS, Lekshmi NM, Pazhayamadom DG (2015) Can the *Nemipterus japonicus* stocks along Indian coast be differentiated using morphometric analysis? Ind J Mar Sci 44(4)
78. Srihari M, Pradhan SK, Pavan-Kumar A, Bhushan S, Nayak BB, Sreekanth GB, Abidi ZJ (2020) Morphometric and meristic analyses of Randall's threadfin bream (*Nemipterus randalli*) Russell, 1986 along the Indian coast. Ind J Fish 67(4):143–148
79. Teacher AG, André C, Jonsson PR, Merilä J (2013) Oceanographic connectivity and environmental correlates of genetic structuring in Atlantic herring in the Baltic Sea. Evolu appli 6(3):549–567
80. Teimori A, Khajooei A, Motamedi M, Hesni MA (2019) Characteristics of sagittae morphology in sixteen marine fish species collected from the Persian Gulf: Demonstration of the phylogenetic influence on otolith shape. Reg Stu Mar Sci 29:100661
81. Tracey SR, Lyle JM, Duhamel G (2006) Application of elliptical Fourier analysis of otolith form as a tool for stock identification. Fish Res 77(2):138–147
82. Turan C (2004) Stock identification of Mediterranean horse mackerel (*Trachurus mediterraneus*) using morphometric and meristic characters. ICES J Mar Sci 61(5):774–781

83. Turan C (1999) A note on the examination of morphometric differentiation among fish populations: the truss system. *Turk J Zool* 23(3):259–264
84. Tuset VM, Rosin PL, Lombarte A (2006) Sagittal otolith shape used in the identification of fishes of the genus *Serranus*. *Fish Res* 81(2–3):316–325
85. Uiblein F, Heemstra PC (2010) A taxonomic review of the Western Indian Ocean goatfishes of the genus *Upeneus* (Family Mullidae), with descriptions of four new species. *Smi Bulle* 11:35–71
86. Urbanek S (2014) jpeg: Read and write JPEG images. R package version 0.1–8. Available: <http://CRAN.R-project.org/package=jpeg>
87. Véron M, Duhamel E, Bertignac M, Pawlowski L, Huret M (2020) Major changes in sardine growth and body condition in the Bay of Biscay between 2003 and 2016: temporal trends and drivers. *Prog Oce* 182:102274
88. Vignon M, Morat F (2010) Environmental and genetic determinant of otolith shape revealed by a non-indigenous tropical fish. *Mar Ecol Prog Ser* 411:231–241
89. Vignon M (2012) Ontogenetic trajectories of otolith shape during shift in habitat use: Interaction between otolith growth and environment. *J Exp Mar Biol Ecol* 420:26–32
90. Vivekanandan E, Srinath M, Pillai VN, Immanuel S, Kurup KN (2003) Marine fisheries along the southwest coast of India. *World Fish*
91. Wujdi A, Setyadji B, Nugroho SC (2017) Preliminary stock structure study of skipjack tuna (*Katsuwonus pelamis*) from south java using otolith shape analysis. *Indian Ocean Tuna Commission P*:19–42

Figures

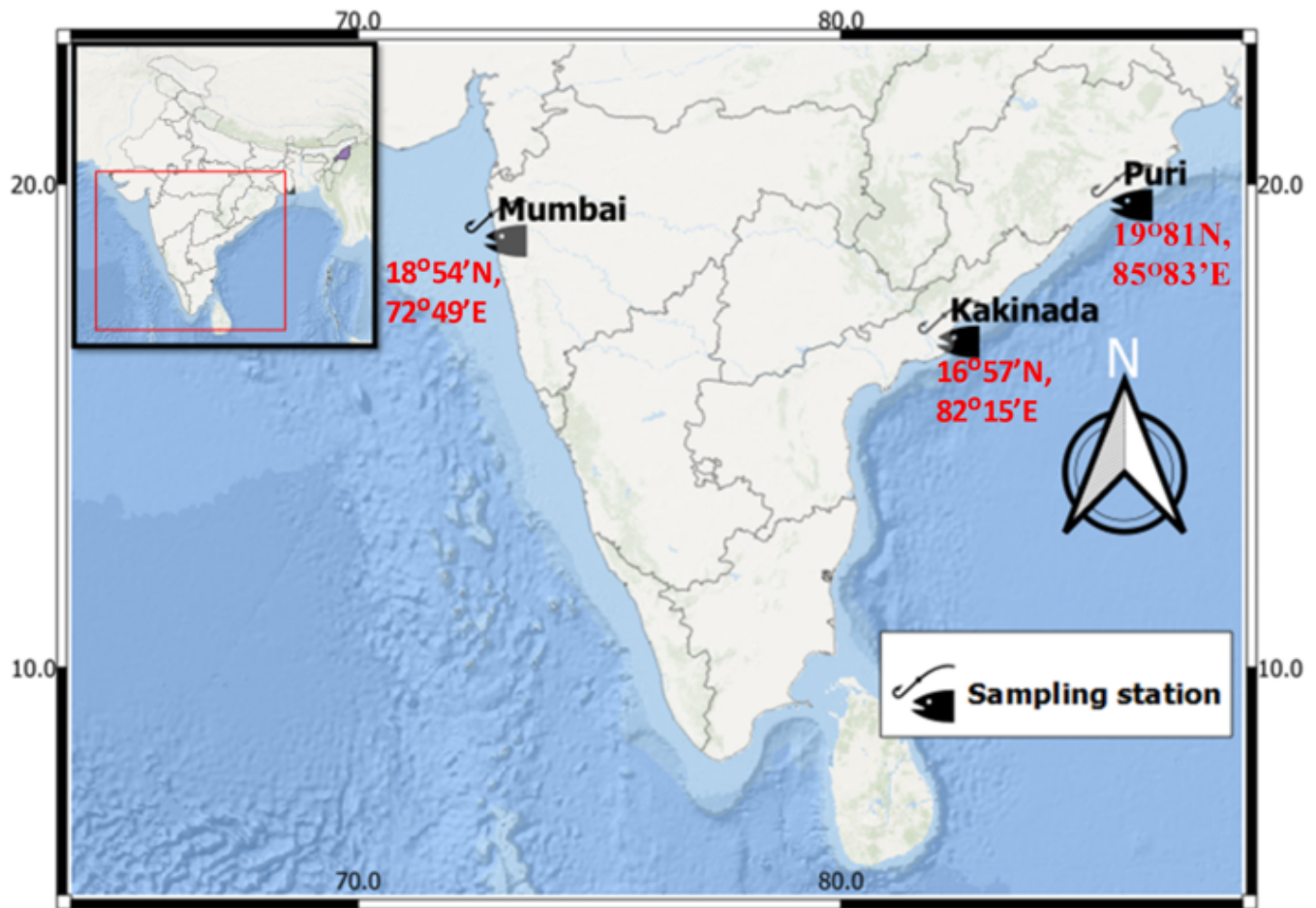


Figure 1

Map showing the sampling locations of *Upeneus vittatus* along the Indian coast with geographic coordinates (Mumbai, Kakinada, Puri).

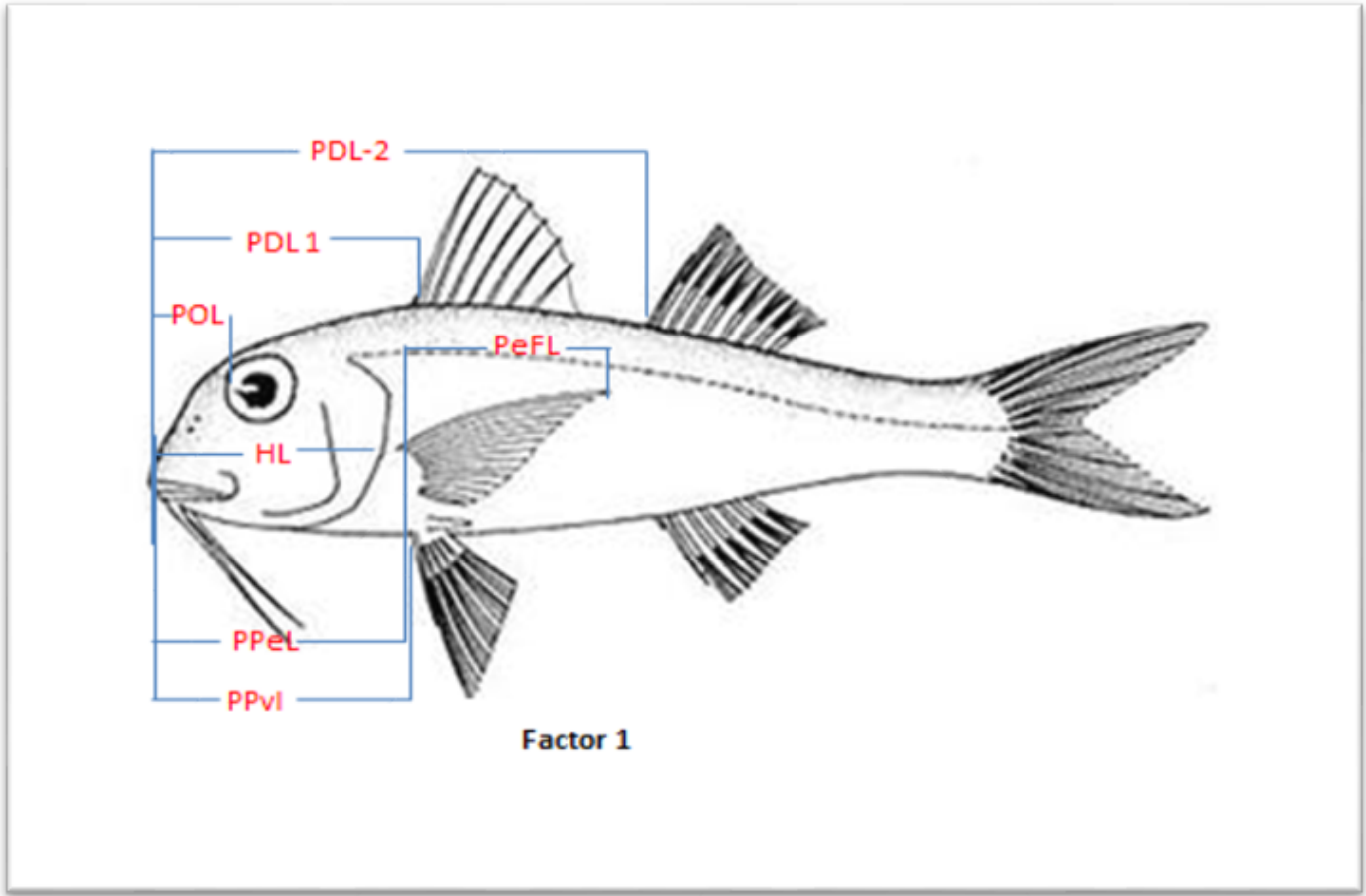


Figure 2

Distance with meaningful loading (above 0.6) on the first factor in morphometric analysis.

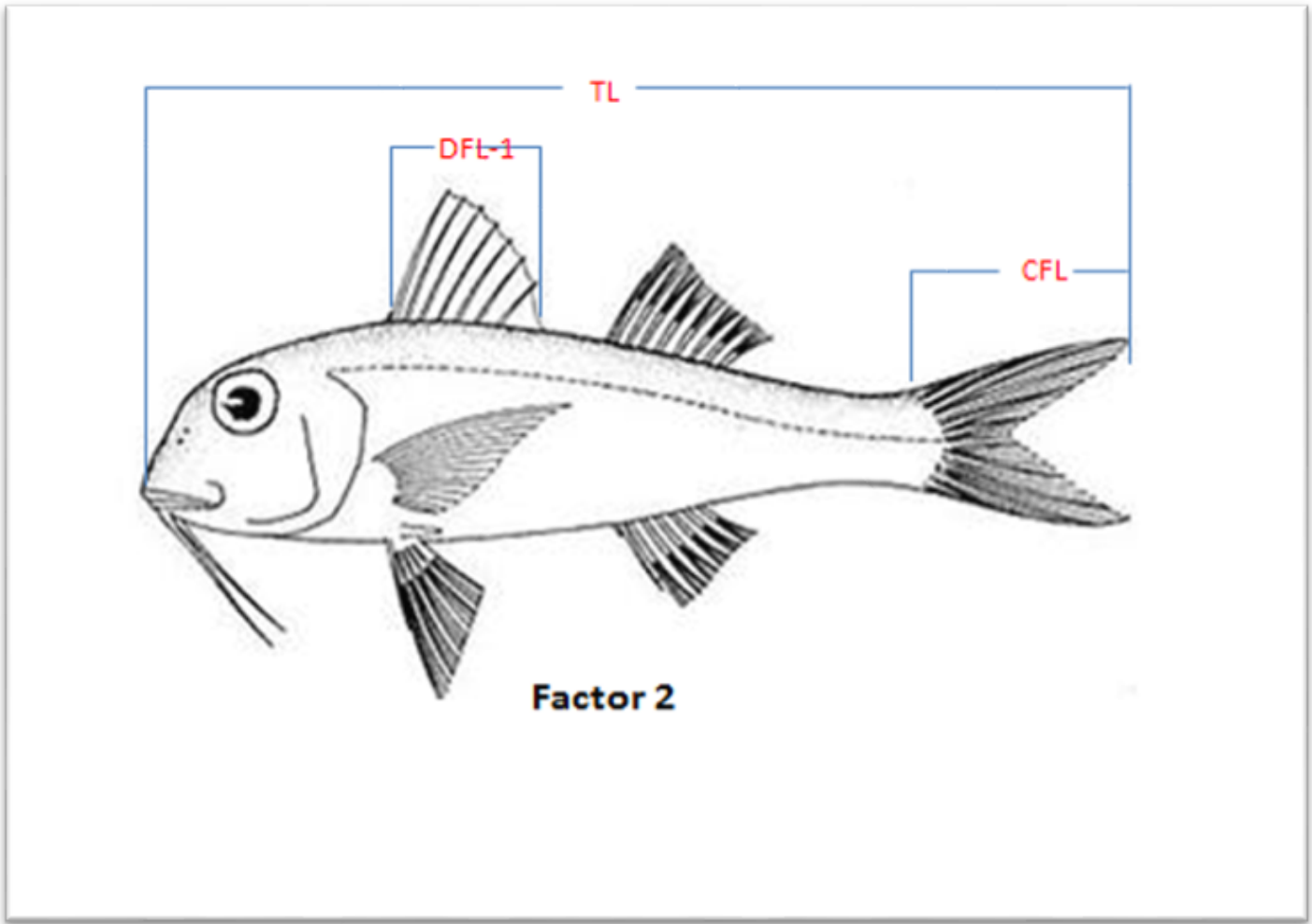


Figure 3

Distance with meaningful loading on the second factor in morphometric analysis.

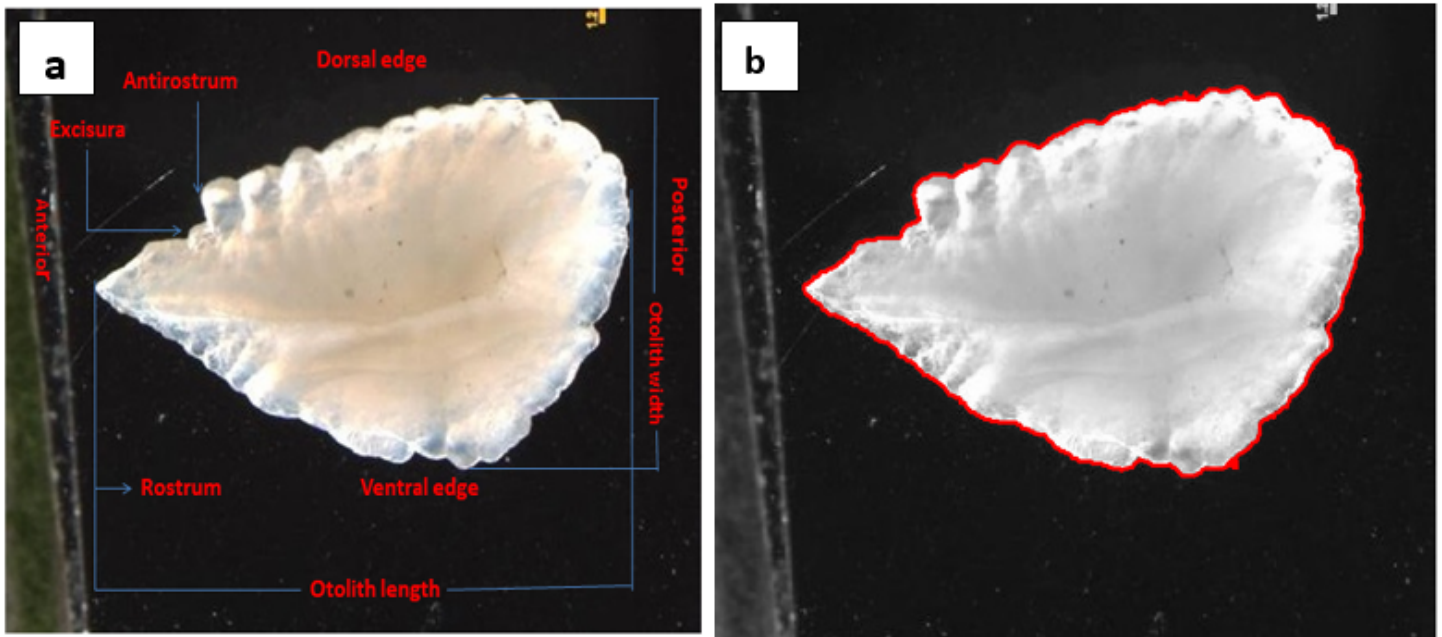


Figure 4

(a) Left sagittal otolith of *U. vittatus* with distal morphological terminology, (b) Otolith with detected outline (marked red line) by ShapeR package for shape analysis.

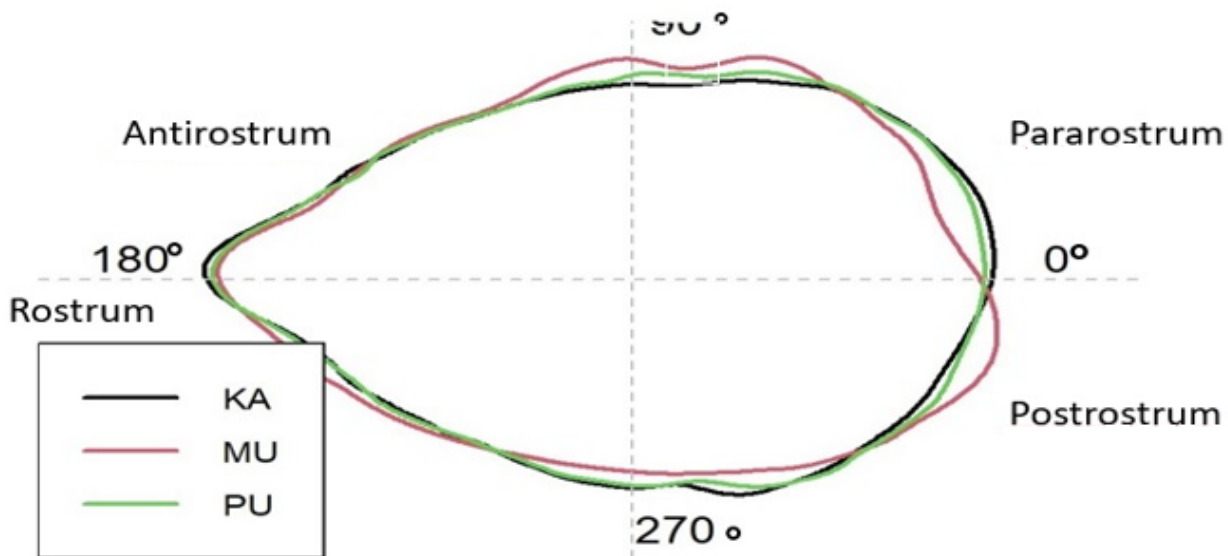


Figure 5

Mean otolith shapes of *U. vittatus* based on Wavelet reconstruction from three locations. Degrees (°) represent angles on polar coordinates. Information about the populations codes (KA: Kakinada; MU: Mumbai; PU: Puri).

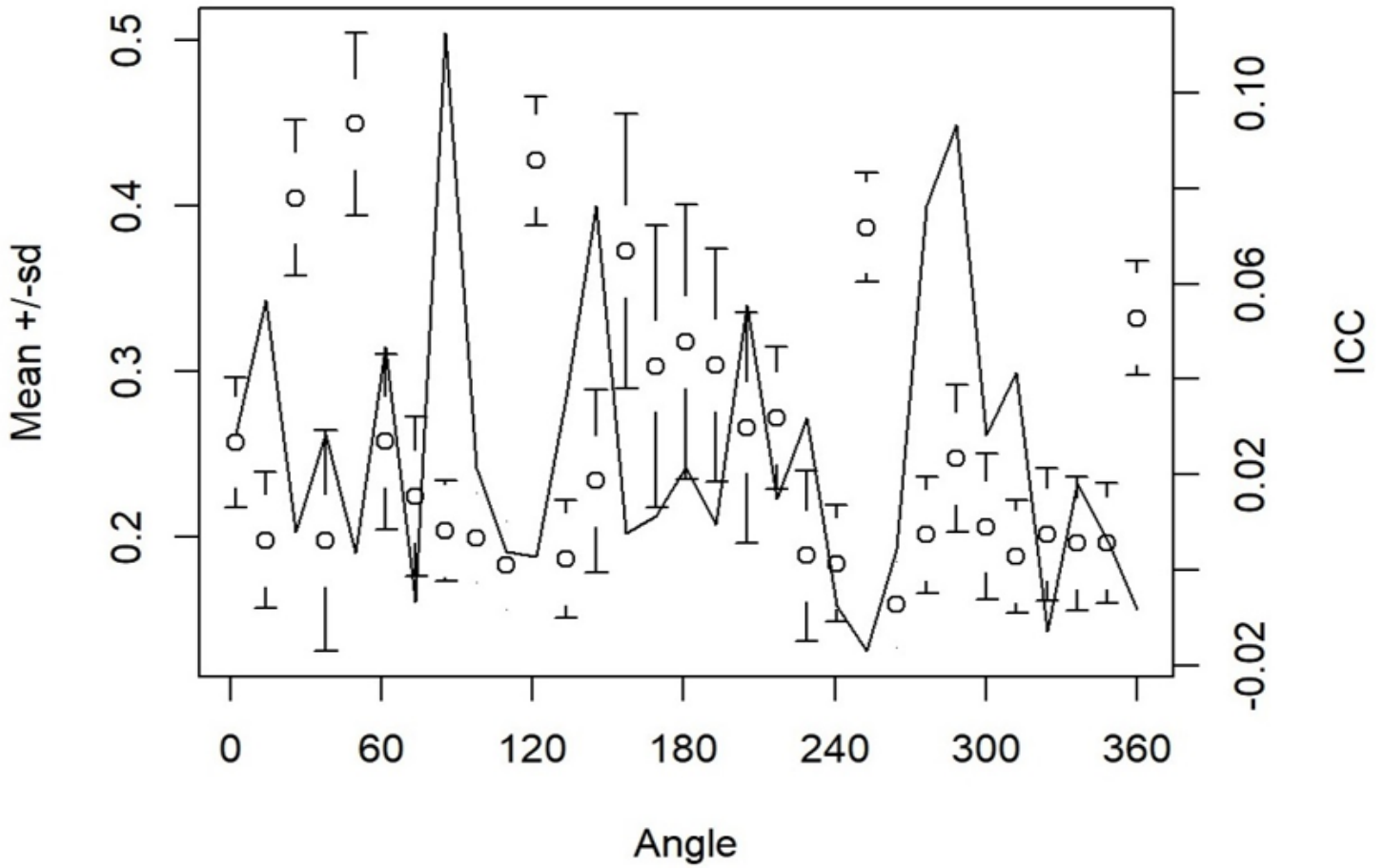


Figure 6

Mean and standard deviation (sd) of the Wavelet coefficients for all combined otoliths and the proportion of variance between *U. vittatus* populations or the intraclass correlation (ICC). The horizontal axis shows angle in degrees (°) as unit based on polar coordinates. Black solid line represents the intraclass correlation.

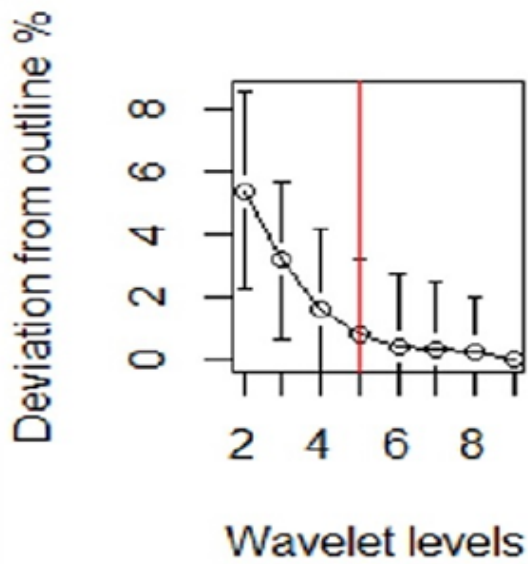


Figure 7

Quality of Wavelet levels reconstruction. The red vertical line shows the levels of Wavelet transform required to achieve 98.5% of precision in the otolith contour modelling of *U. vittatus*.

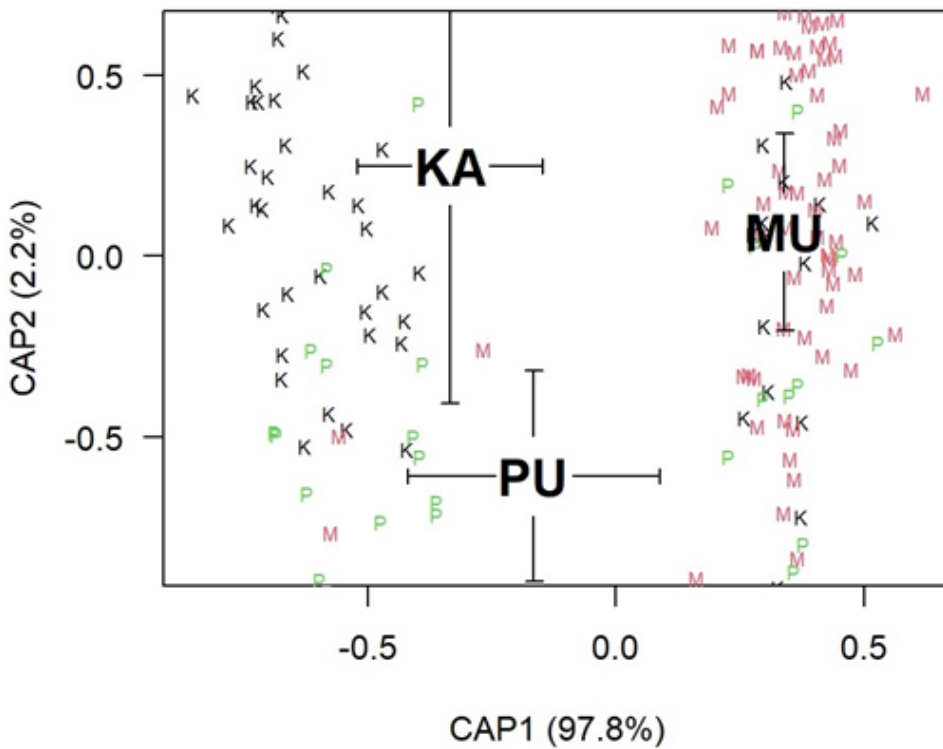


Figure 8

Canonical analysis of principal coordinates (CAP) of the Wavelet coefficients from three sampling populations along the Indian coast is given. CAP1 and CAP2 represent canonical scores on the first two discriminating axes

for each sampling location. Black letters indicate the mean canonical coordinates for each population, Kakinada (KA), Mumbai (MU) and Puri (PU). Small letters represent individual fish. Mean canonical coordinates is surrounded by interval, present one standard error (mean +/- 1SE) for the potential stock.